ELSEVIER

Catalysis Today 32 (1996) 21–28

CATALYSIS TODAY

Some kinetic aspects of unsteady-state partial oxidation reactions Dynamic processes on metal oxide surfaces

Yuri I. Pyatnitsky *, Nina I. Ilchenko

Pisarzhevsky Institute of Physical Chemistry, Kiev, 252039, Ukraine

Abstract

It is shown that steady-state kinetic data do not allow the discrimination between the redox and associated mechanisms of the partial oxidation reactions. A discrimination between these mechanisms was performed using transient experiments. The obtained rate expressions are in agreement with experimental kinetic data for catalytic partial oxidation of *o*-xylene.

An influence of the conjugate oxidation of a catalyst surface on dynamics and kinetics of the heterogeneous catalytic oxidative reactions is considered. Computing simulation of methane oxidative coupling of methane reaction at lowered temperature and elevated pressure has been performed. It showed that the reaction order with respect to oxygen exceeding unity is consistent with the chain branching mechanism of the reaction in the presence of $TiSi_2$ and TiB_2 and showed the important role of the branching chain cycles in the low-temperature OCM reaction at elevated pressure.

Keywords: Kinetic aspects; Unsteady-state; Partial oxidation; Dynamic processes; Metal oxide surfaces

1. Introduction

Many metal oxides are efficient catalysts for oxidation reactions. Every oxidation reaction (or a separate group of reactions) has its specific features. Meanwhile, the formal schemes of the various oxidation reactions are similar to a certain extent [1]. This has given reason to believe that there are some common approaches to the kinetics and dynamics of oxidation reactions. In this report we set forth some approaches derived from kinetic analysis of oxidation reaction schemes.

2. Typical mechanisms of heterogeneous oxidation reactions over metal oxides

The simple redox mechanism of oxidation reactions over metal oxide catalysts is well-known. According to this mechanism, the final reaction products R_1, R_2,...R_i are formed in the step of a reductant R interaction with oxidized catalyst sites, ZO. The decrease of surface oxygen is compensated by the gas-phase oxygen reaction with the reduced catalyst sites, Z.

This 'two-step' redox mechanism may be presented as

$$Z + O_2 \underset{k_0}{\rightarrow} ZO_2 \overset{Z}{\rightarrow} 2ZO$$

$$R + ZO \underset{k}{\rightarrow} ROZ \overset{2(\nu-1)ZO}{\rightarrow} R_1, R_2 ... R_i \qquad (1)$$

* Corresponding author.

PII S0920-5861(96)00093-4

where k_0 and k are rate constants, ν is the mean number of oxygen molecules consumed for the oxidation of one molecule R.

Thus, the redox mechanism consists of the separate interaction of the reagents, R and O_2, with an oxide catalyst surface. Therefore, the rate of the catalyst surface reduction by reductant R, r_{red}, should be equal to the rate of a steady-state catalytic reaction, r, at the same catalyst surface coverage by oxygen, θ. This kinetic feature has been observed in a number transient dynamic studies of the oxidation reactions over metal oxides.

For example, the comprehensive transient experiment dynamic studies combined with the steady-state measurements for hydrogen oxidation over F_2O_3, Co_3O_4, MnO_2, ZnO, Cr_2O_3 and CuO [2,3] have shown that the values of r and r_{red} are close at the same amount of surface oxygen [2,3]. The same is true for the reactions of selective oxidation of *o*-xylene and naphthalene over V_2O_5-K_2SO_4-SiO_2. Moreover, not only the overall reaction rates, but also the reaction product selectivities coincide in the transient dynamic and steady-state experiments at the same values of θ [4,5]. Additional evidence of the redox mechanism (1) is the correlation between concentration of V^{4+} ions in the V_2O_5-K_2SO_4-SiO_2 catalyst and O_2/*o*-xylene ratio under steady-state reaction conditions [6].

The other typical mechanism of oxidation reaction is the mechanism which includes, together with direct surface oxidation with oxygen, the conjugation of desorption of the reaction products with surface reoxidation by oxygen. This mechanism was called an associated mechanism by Boreskov [7], a conjugate oxidation mechanism [8], or a mechanism with complex (conjugate) surface reoxidation [9,10].

In the case of an associated mechanism, the steady-state rate of a reaction is higher than that of the rate of R conversion to reaction products. This takes place, for example, at low-temperature oxidation of alkanes and CO over ZnO [8]. No gas-phase product formation has been observed in the reaction between *o*-xylene and the oxidized surface of a V_2O_5-TiO_2 catalyst at 603 K although steady-state catalytic oxidation of *o*-xylene proceeds with almost 100% conversion under the same conditions [11].

It is suggested that the reason for the lowered rates of product formation in the absence of oxygen is the formation of strong adsorbed intermediates in the reaction of R with oxidized catalyst surface. If R is CO, these intermediates are the surface carbonates Z_2O_2CO, which are bonded with partly reduced catalyst sites [8]. Their spontaneous decomposition to CO_2 is slow at relatively low temperatures. However, the CO_2 desorption can be sharply increased in the presence of oxygen due to conjugation of the exothermic step of desorption with the endothermic step of the oxidation of reduced sites by oxygen [8]. This may be presented by the following scheme

$$Z_2O_2CO + O_2 \rightarrow ZO_2 + ZO + CO_2 \qquad (2)$$

In the case of the selective oxidation of *o*-xylene, the strong bonded adsorbed species are also the salt-like compounds such as the surface phthalate and maleate complexes [11].

As seen, to discriminate between the above two mechanisms, transient dynamic experiments are used, first of all. The steady-state experiments do not provide such certain information. Indeed, in the case of the simple two-step redox mechanism (1), if ZO is assumed to be the most abundant surface intermediate, its surface coverage θ is given by

$$\theta = (k_0/\nu)P_{O_2} \Big/ \left((k_0/\nu)P_{O_2} + kP_R\right) \qquad (3)$$

Thus, we can obtain a rate equation of the Mars and Van Krevelen type [12]:

$$r = kP_R\theta = \frac{(k_0/\nu)P_{O_2}kP_R}{(k_0/\nu)P_{O_2} + kP_R} \qquad (4)$$

where P_{O_2} and P_R are the partial pressures of oxygen and oxidized reactant R, respectively.

The coefficient ν depends on the reaction product selectivities, S_i, and stoichiometric coefficients with respect to molecular oxygen, ν_i,

in reactions of conversion of R to R_1, R_2... R_i as follows

$$\nu = \nu_1 S_1 + \nu_2 S_2 + ... + \nu_i S_i \quad (5)$$

The validity of Eq. (4) was demonstrated in many works for the various oxidation reactions over oxide catalysts (see, for example, [1]).

However, the same form of the rate equation can also be obtained for the associated mechanism. To show this, let us consider the simple scheme of the associated mechanism:

$$Z + O_2 \xrightarrow[k_0]{Z} ZO_2 \rightarrow 2ZO$$

$$R + ZO \xrightarrow[k_1]{} R_1Z \xrightarrow{(2\nu+\mu-1)ZO} \mu Z_2O_2CO$$

$$Z_2O_2CO \xrightarrow[k_2]{O_2} CO_2 + ZO_2 + ZO \quad (6)$$

where μ is the number of carbon atoms in the molecule R.

If ZO and Z_2OCO_2 are assumed to be the most abundant surface intermediates, then the oxygen fractional coverage is

$$\theta = \frac{(k_0/\alpha)P_{O_2}}{(k_0/\alpha)P_{O_2} + kP_R} \quad (7)$$

where

$$\alpha = \nu + \mu[(2k_0/k_2) - 1] \quad (8)$$

Thus, the rate of the reaction becomes

$$r = kP_R\theta = \frac{(k_0/\alpha)P_{O_2}kP_R}{(k_0/\alpha)P_{O_2} + kP_R} \quad (9)$$

If we include in scheme (6) the following step

$$R_1Z + O_2 \xrightarrow[k_3]{} ZO_2 + R_1 \quad (10)$$

then the coefficient α is

$$\alpha = \nu + [(k_0/k_3) - 1]S_1 + \mu[(2k_0/k_2 - 1]S_2 \quad (11)$$

It is clear that the kinetic Eqs. (4) and (6) are nondistinctive kinetically for nonselective reactions. For selective reactions, the difference between these equations is not significant because both coefficients ν and α are linear functions of the selectivities. Besides, if average values of ν and α are used to linearize the kinetic model, the form of Eqs. (4) and (6) becomes the same.

In principle, the mechanism of the oxidation reaction may be the sum of both the redox and associated mechanisms. Their relative contribution depends on the catalyst type as well as the temperature [8].

3. Unsteady-state dynamic features of oxidation reactions over metal oxides

As mentioned above, the transient experiments with an investigation of the dynamics of reagent interaction with a catalyst allows the discrimination between the redox and associated mechanisms. As examples of both mechanism types, we will consider the reactions of the partial oxidation of toluene and *o*-xylene over V_2O_5 and V_2O_5-TiO_2 catalysts.

The transient dynamic experiments were performed in a differential flow reactor at 548 K. The catalysts were V_2O_5 (0.5–1 mm, 5.5 m^2/g, 1.5 g) and V_2O_5-TiO_2-SiO_2 (0.25–0.5 mm, 8.2 m^2/g, 1.0 g). The catalysts were first treated with a 21 vol% $O_2 + N_2$ mixture at 548 K for 2 h. Then, the reductive Re + He mixture (the R concentrations were 2.9 and 0.7 vol% for toluene and *o*-xylene, respectively) was exposed to the oxidized catalyst and chromatographically analyzed at the reactor outlet. After some time, the R + He mixture was replaced by 21 vol% O_2 + N_2 and the gas phase from the reactor was again analyzed. The results for V_2O_5-TiO_2-SiO_2 are shown in Fig. 1 and Fig. 2. Similar unsteady-state dynamic features were observed in the presence of V_2O_5.

The data in Fig. 1 and Fig. 2 indicate that the toluene to benzaldehyde and *o*-xylene to *o*-toluene aldehyde reactions obey the redox type mechanism (1), while more oxidized products, maleic anhydride and CO_2 in the toluene oxidation, and phthalic anhydride and CO_2 in the *o*-xylene oxidation, are formed mainly via the mechanism with the conjugate surface oxida-

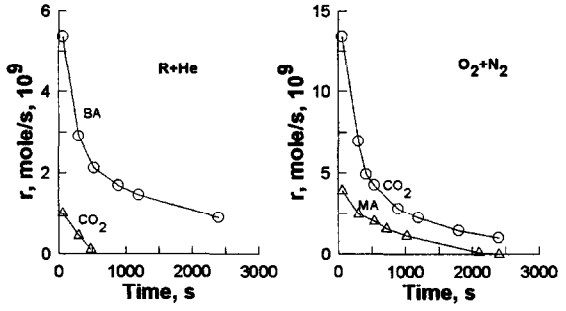

Fig. 1. Rates of benzaldehyde (BA), maleic anhydride (MA) and CO_2 formation in the transient experiments on V_2O_5-TiO_2-SiO_2, R = toluene.

tion. The probable mechanism of conjugate oxidation may be similar to the above mechanisms (2) or (10).

Based on the data of the unsteady-state runs, we have estimated the rate constants of the steps of conjugate surface oxidation in the *o*-xylene $+ O_2/V_2O_5$-TiO_2-SiO_2 system. It was speculated that the decomposition of the corresponding surface species are first order with respect to the adsorbed species and the gas-phase oxygen. Then, the dependence of the intermediate fractional coverage θ_i on time is

$$-\mathrm{d}\theta_i/\mathrm{d}t = \left(k_i P_{O_2}/L_0\right)\theta_i \qquad (12)$$

where k_i is the rate constant, mol/m^2 s Pa, and L_0 the total surface concentration of active sites, mol/m^2.

Because the rate of the R_i product formation is in direct proportion with the θ value, we can obtain

$$\ln\left(\theta_i/\theta_i^0\right) = \ln\left(r_i/r_i^0\right) = -\left(k_i P_{O_2}/L_0\right)t \qquad (13)$$

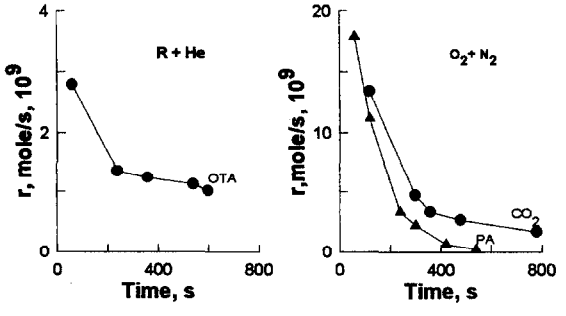

Fig. 2. Rates of *o*-toluene aldehyde (OTA), phthalic anhydride (PA) and CO_2 formation in the transient experiments on V_2O_5-TiO_2-SiO_2, R = *o*-xylene.

Using this equation, we have found that the rate constant is $4.7 \cdot 10^{-12}$ mol/m^2 s Pa for CO_2 and $7.2 \cdot 10^{-12}$ mol/m^2 s Pa for phthalic anhydride. These values are used below to treat the steady-state kinetics of *o*-xylene oxidation.

4. The steady-state kinetic model

Taking into account the results of the transient dynamic experiments and the literature data [9,10,13–16], the probable mechanism of the *o*-xylene conversion to OTA, PA and CO_2 can be presented as

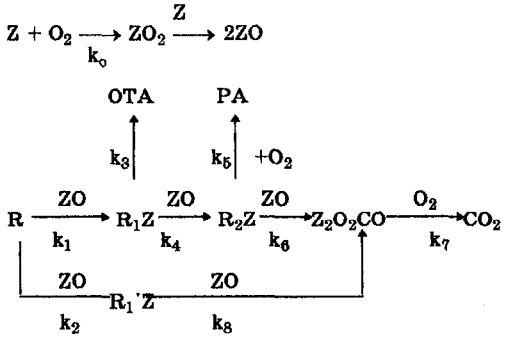

(14)

It is assumed that there are two parallel pathways on the catalyst surface. One begins from the attack of the methyl group in the *o*-xylene molecule, the other from the attack of the aromatic ring. Another assumption is the first order with respect to ZO species in the surface oxidation reactions. If also the ZO, ZR'_1, ZR_2 and Z_2O_2CO are assumed to be the most abundant surface intermediates with fractional coverage θ, θ'_1, θ_2 and θ_3, respectively, we can deduce for the steady state regime:

$$r_0 + r_5 + r_7 = (\nu_1 S_1 + \nu_2 S_2 + \nu_3 S_3) r \qquad (15)$$

$$r_0 = k_0 P_{O_2}(1 - \theta - \theta'_1 - \theta_2 - 2\theta_3) \qquad (16)$$

$$r = (k_1 + k_2) P_R \theta = k P_R \theta \qquad (17)$$

$$r_5 = k_5 P_{O_2} \theta_2 \qquad (18)$$

$$r_7 = k_7 P_{O_2} \theta_3 \qquad (19)$$

$$r_8 = k_8 P_R \theta'_1 \qquad (20)$$

$$S_1 = (k_1/k)/[1 + n_1\theta] \qquad (21)$$

$$S_2 = (k_1/k)[n_1\theta/(1+n_1\theta)][1/(1+n_2\theta)] \quad (22)$$

$$S_3 = (k_1/k)[n_1\theta/(1+n_1\theta)][n_2\theta(1+n_2\theta)] + (k_2/k) \quad (23)$$

$$\theta_2 = kP_R\theta S_2[1/(k_5P_{O_2})] \quad (24)$$

$$\theta_3 = kP_R\theta S_3[\mu/(k_7P_{O_2})] \quad (25)$$

$$\theta_1' = k_2P_R/k_8 \quad (26)$$

where $n_1 = k_4/k_3$ and $n_2 = k_6/(k_5P_{O_2})$. The system of Eqs. (15)–(26) is the compact description of the non-linear kinetic model of the reaction. Computing optimization of kinetic parameters showed satisfactory agreement between the calculated and the experimental data (Fig. 3).

We propose that a similar approach may be generalized to explain kinetics of other reactions of organic compound oxidation, not only of aromatic hydrocarbons.

Scheme (14) describes the reaction at low conversions of the oxidized reagent R when the secondary reactions of the R_1, R_2... R_i products can be neglected. At high conversions, Scheme (14) should be complicated by including the following reactions:

$$R_j + ZO \xrightarrow[k_j]{} R_{j+1}Z \rightarrow R_{j+1},\ R_{j+2}...R_i$$

The reactions of partial oxidation of organic compounds, viewed as a specific case of competitive reaction, may show an amazing 'mixture effect': the form of the rate equations of the $R + O_2$ and $R_j + O_2$ reactions are the same [17]. This kinetic feature simplifies the derivation of kinetic equations for common parallel-consecutive reaction schemes [16].

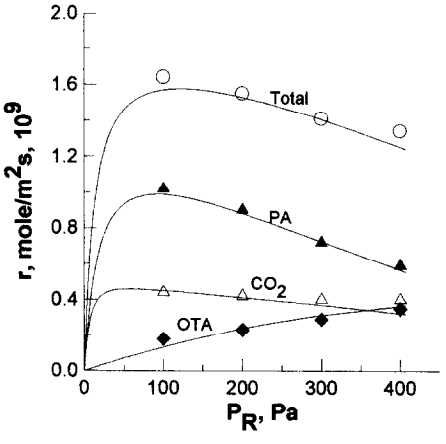

Fig. 3. Dependence of the rates of *o*-xylene oxidation and product formation over V_2O_5-TiO_2-SiO_2 on *o*-xylene partial pressure at 548 K, 21.3 kPa O_2. Curves were calculated at $\nu_1 = 1$, $\nu_2 = 3$, $\nu_3 = 10.5$, $\mu = 8$, $n_1 = 80$, $k_0 = 2.1 \cdot 10^{-13}$, $k_1 = 1.2 \cdot 10^{-10}$, $k_2 = 4.1 \cdot 10^{-11}$, $k_5 = 7.2 \cdot 10^{-12}$, $k_6 = 7.7 \cdot 10^{-8}$, $k_7 = 4.7 \cdot 10^{-12}$, $k_8 = 4.0 \cdot 10^{-8}$ (k_0, k_1, k_2, k_5 and k_7 in mol/m^2 s Pa, k_6 and k_8 in mol/m^2 s).

5. Heterogeneous-homogeneous oxidative coupling of methane

Above, we have considered the schemes of heterogeneous oxidation reactions. The reaction of oxidative coupling of methane (OCM) is a heterogeneous-homogeneous reaction type. As generally accepted, oxide catalysts are the producers of methyl radicals which react in the gas phase. Kinetic computer models based on the free radical mechanisms have been developed in some recent studies, among others, in [18–24].

In the present paper, we consider the oxygen concentration influence on the OCM reaction at relatively low (below 873 K) temperature and elevated (higher 0.1 MPa) pressure. Under these conditions, the OCM reaction has been performed in the presence of transition metal borides, silicides, nitrides and carbides the surface layers of which contain the oxidized forms of parent metals [25,26]. It was shown, in particular, that the reaction order with respect to oxygen often exceed unity. Another effect is the strong reaction rate dependence on pressure: this is hard to explain in terms of common schemes for heterogeneous catalytic oxidative reactions. The reaction rate is very small for 0.1 MPa, and as pressure increases up to 0.2–0.3 MPa the reagent conversion reaches high values. To explain these effects, we have performed a computer simulation based on the reactions listed in Table 1. The kinetic parame-

Table 1
The mechanism used for the OCM reaction kinetic simulation [a]

No.	Reaction	A	n	E/R
Homogeneous reactions				
27	$CH_4 + O_2 \rightarrow CH_3 + HO_2$	$4.03 \cdot 10^7$		28 640
28	$CH_4 + H \rightarrow CH_3 + H_2$	$2.25 \cdot 10^{-2}$	3.00	4406
29	$CH_4 + O \rightarrow CH_3 + OH$	$1.02 \cdot 10^3$	1.50	4330
30	$CH_4 + OH \rightarrow CH_3 + H_2O$	$1.93 \cdot 10^{-1}$	2.40	1060
31	$CH_4 + HO_2 \rightarrow H_2O_2 + CH_3$	$1.81 \cdot 10^5$		9350
32	$2\,CH_3 \rightarrow C_2H_6$	$1.09 \cdot 10^9$	−0.64	
33	$CH_3 + O_2 \rightarrow CH_3O_2$	$9.03 \cdot 10^{52}$	−15.01	8567
34	$CH_3 + O_2 \rightarrow CH_3O + O$	$1.99 \cdot 10^{12}$	−1.57	14 710
35	$CH_3 + O_2 \rightarrow CH_2O + OH$	$5.40 \cdot 10^7$		12 200
36	$CH_3 + HO_2 \rightarrow CH_3O + OH$	$1.99 \cdot 10^7$		
37	$CH_3 + H_2O_2 \rightarrow CH_4 + HO_2$	$1.20 \cdot 10^4$		−300
38	$CH_3 + C_2H_6 \rightarrow CH_4 + C_2H_5$	$5.48 \cdot 10^{-7}$	4	4169
39	$CH_3 + CH_2O \rightarrow CH_4 + CHO$	$5.54 \cdot 10^{-3}$	2.81	2950
40	$C_2H_6 + O_2 \rightarrow C_2H_5 + HO_2$	$4.03 \cdot 10^7$		25 600
41	$C_2H_6 + H \rightarrow C_2H_5 + H_2$	$5.54 \cdot 10^{-4}$	3.5	2600
42	$C_2H_6 + O \rightarrow C_2H_5 + OH$	$1.20 \cdot 10^6$	0.6	3680
43	$C_2H_6 + OH \rightarrow C_2H_5 + H_2O$	$8.85 \cdot 10^3$	1.04	913
44	$C_2H_6 + HO_2 \rightarrow H_2O_2 + C_2H_5$	$2.95 \cdot 10^5$		7520
45	$C_2H_4 + CH_3 \rightarrow C_2H_3 + CH_4$	$6.62 \cdot 10^{-6}$	3.7	4780
46	$C_2H_4 + H \rightarrow C_2H_3 + H_2$	1.32	2.53	6160
47	$C_2H_4 + O \rightarrow CH_3 + CHO$	$1.32 \cdot 10^2$	1.55	215
48	$C_2H_4 + OH \rightarrow C_2H_3 + H_2O$	$1.57 \cdot 10^{-2}$	2.75	2100
49	$CH_3O_2 \rightarrow CH_3 + O_2$	$7.23 \cdot 10^{42}$	−10.02	16 731
50	$CH_3O_2 + CH_3 \rightarrow 2\,CH_3O$	$2.41 \cdot 10^7$		
51	$CH_3O + M \rightarrow CH_2O + H + M$	$3.91 \cdot 10^{31}$	−6.65	16 740
52	$CH_3O + HO_2 \rightarrow CH_2O + H_2O_2$	$3.01 \cdot 10^5$		
53	$CH_2O + O_2 \rightarrow HO_2 + CHO$	$2.05 \cdot 10^7$		19 600
54	$CH_2O + H \rightarrow H_2 + CHO$	$2.19 \cdot 10^2$	1.77	1510
55	$CH_2O + O \rightarrow CHO + OH$	$1.87 \cdot 10^7$		1550
56	$CH_2O + OH \rightarrow CHO + H_2O$	$3.43 \cdot 10^3$	1.18	−225
57	$CH_2O + HO_2 \rightarrow H_2O_2 + CHO$	$1.99 \cdot 10^6$		5870
58	$C_2H_5 \rightarrow C_2H_4 + H$	$4.90 \cdot 10^3$	1.19	18 772
59	$C_2H_5 + H_2O_2 \rightarrow C_2H_6 + HO_2$	$8.73 \cdot 10^3$		490
60	$C_2H_5 + HO_2 \rightarrow CH_3 + CH_2O + OH$	$2.41 \cdot 10^7$		
61	$C_2H_5 + O_2 \rightarrow C_2H_4 + HO_2$	$8.43 \cdot 10^5$		1950
62	$C_2H_5 + CH_2O \rightarrow C_2H_6 + CHO$	$5.49 \cdot 10^{-3}$	2.81	2950
63	$C_2H_3 + H_2 \rightarrow C_2H_4 + H$	$3.01 \cdot 10^{-2}$	2.63	4298
64	$C_2H_3 + O_2 \rightarrow C_2H_2 + HO_2$	$1.20 \cdot 10^5$		
65	$C_2H_3 + HO_2 \rightarrow OH + CH_3 + CO$	$3.01 \cdot 10^7$		
66	$C_2H_3 + H_2O_2 \rightarrow C_2H_4 + HO_2$	$1.20 \cdot 10^4$		−300
67	$C_2H_3 + CH_2O \rightarrow C_2H_4 + CHO$	$5.42 \cdot 10^{-3}$	2.81	2950
68	$CHO + O_2 \rightarrow HO_2 + CO$	$5.12 \cdot 10^7$		850
69	$CO + OH \rightarrow H + CO_2$	$6.74 \cdot 10^4$		$E/R = -0.0009T$
70	$CO + HO_2 \rightarrow OH + CO_2$	$1.51 \cdot 10^8$		11 900
71	$CO_2 + H \rightarrow CO + OH$	$1.51 \cdot 10^8$		13 300
72	$H + O_2 \rightarrow OH + O$	$1.69 \cdot 10^{11}$	−0.9	8750
73	$H + O_2 + M \rightarrow HO_2 + M$	$6.42 \cdot 10^6$	−1	
74	$O + H_2 \rightarrow OH + H$	$1.08 \cdot 10^{-2}$	2.8	2980
75	$OH + H_2 \rightarrow H + H_2O$	6.38	2	1490
76	$HO_2 + H \rightarrow 2OH$	$1.69 \cdot 10^8$		440
77	$HO_2 + H \rightarrow H_2 + O_2$	$6.62 \cdot 10^7$		1070
78	$HO_2 + O \rightarrow OH + O_2$	$1.75 \cdot 10^7$		−200
79	$HO_2 + OH \rightarrow H_2O + O_2$	$1.45 \cdot 10^{10}$	−1	
80	$2\,HO_2 \rightarrow H2O2 + O_2$	$1.81 \cdot 10^6$		

Table 1 (continued)

No.	Reaction	A	n	E/R
81	$H_2O_2 + M \rightarrow 2OH + M$	$1.29 \cdot 10^{27}$	−4.86	26795
82	$H_2O_2 + O_2 \rightarrow 2\,HO_2$	$5.42 \cdot 10^{7}$		20000
83	$H_2O_2 + H \rightarrow H_2 + HO_2$	$4.82 \cdot 10^{7}$		4000
84	$H_2O_2 + H \rightarrow H_2O + OH$	$2.41 \cdot 10^{7}$		2000
85	$H_2O_2 + O \rightarrow OH + HO_2$	9.64	2	2000
86	$H_2O_2 + OH \rightarrow H_2O + HO_2$	$1.75 \cdot 10^{6}$		160
Heterogeneous reactions				
87	$CH_4 + ZO \rightarrow CH_3 + ZOH$			
87′	$2ZOH = H_2O + ZO + Z$			
87′	$2Z + O_2 = 2ZO$			

[a] Rate constants given as $k = At^n\exp(-E/RT)$. Units of k s^{-1}, $m^3/(mol\ s)$ or $m^6/(mol^2\ s)$.

ters of homogeneous reactions were chosen from a kinetic database [27] and were used without any optimization. As in [23], the rate constant of heterogeneous reaction $CH_4 + ZO \rightarrow CH_3 + ZOH$, k_c, was varied so that calculated methane conversion matched the experimental values (the other heterogeneous reactions, presented in Table 1 and needed to close the surface reaction cycle, are assumed to be fast).

The most probable primary reactions of CH_3 radicals with oxygen that compete with the methyl radicals recombination to ethane are reactions (33) and (34). Reaction (33) with subsequent reactions (49), (50), (51) and (3) constitute the unbranched cycle

$$2CH_4 + O_2 = 2CH_2O + 2H_2 \qquad (88)$$

while reaction (34) with reactions (51), (28), (29) and (30) form the branched cycle

$$3CH_4 + O_2 = 2CH_3 + CH_2O + H_2 + H_2O \qquad (89)$$

If the reaction cycle (88) dominates and the reversible step (33) is in equilibrium, the rate of methane consumption is

$$r_{CH_4} = r_{in}S_{C_2} = \frac{r_{in}k_7}{k_7 + k_{27}(k_8/k_{26})P_{O_2}} \qquad (90)$$

where r_{in} is the rate of CH_3 radical initiation, and S_{C_2} selectivity towards ethane.

In contrast, if the branched cycle (89) is abundant and the rate of radical chain initiation, in comparison with the chain branching, is small, then

$$r_{CH_4} = 3r_9 = 3k_9^2/k_7P_{O_2}^2 \qquad (91)$$

(in this case, the value of S_2 is equal to 2/3).

As seen, the branching chain reaction route is more consistent with a reaction order to O_2 exceeding unity. This is confirmed by the computer simulation of oxygen influence on the reaction rate. Fig. 4 demonstrates good agreement between the experimental data, obtained in a stainless steel reactor, and calculated data. The computer simulation shows also the strong dependence of the reaction rate on pressure in agreement with experimental data (Fig. 5).

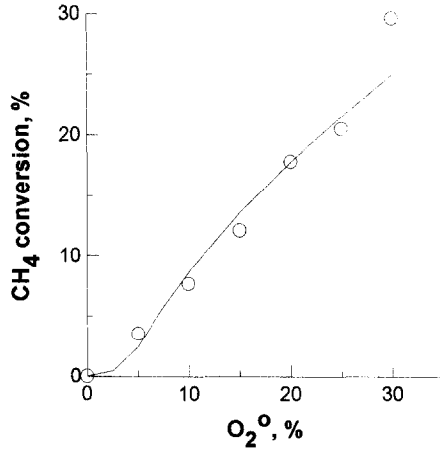

Fig. 4. Dependence of methane conversion in the OCM reaction in the presence of $TiSi_2$ (823 K, 0.35 MPa, 70% CH_4, residence time: 10 s) on inlet oxygen concentration. Curve was calculated using mechanism presented in Table 1 ($k_{87} = 10^{-4}$ s^{-1}).

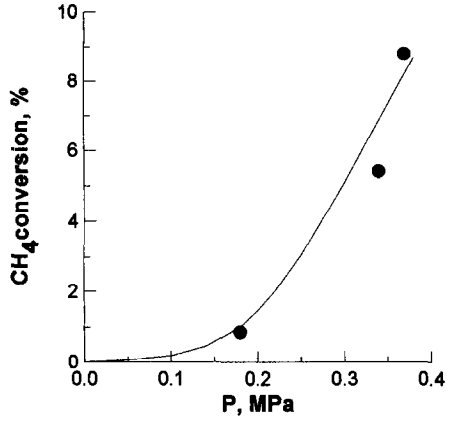

Fig. 5. Dependence of methane conversion in the OCM reaction in the presence of TiB_2 (823 K, 0.35 MPa, 73% CH_4, 27% O_2, residence time: 5 s) on pressure. The curve was calculated using mechanism presented in Table 1 ($k_{87} = 5 \cdot 10^{-5}$ s^{-1}).

Thus, one may suppose that (a) the branching chain reactions play an important role in the low-temperature OCM process at elevated pressure and (b) the catalyst, being the initiator of the chain reaction, is not a major source of methyl radicals. The important role of the chain branching reactions in the high temperature OCM process was indicated before [28]. Meanwhile, the kinetic model, being very poor with respect to heterogeneous steps, does not predict the true value of reaction selectivity. Apparently, the catalyst also interacts with reaction intermediates, changing the final product distribution.

Acknowledgements

The authors gratefully thank Carl A. Udovich (Amoco Corp.) for helpful cooperation and providing the computer facilities. The authors also greatly appreciate the support of the computer research by the Amoco Corporation.

References

[1] G.I. Golodets, Heterogeneous Catalytic Reactions Involving Molecular Oxygen, Elsevier, New York, 1983.
[2] E.A. Mamedov, V.V. Popovsky and G.K. Boreskov, Kinet. Catal., 10 (1969) 852.
[3] G.K. Boreskov, V.V. Popovsky and E.A. Mamedov, Dokl. AN SSSR, 197 (1971) 373.
[4] Yu. Pyatnitsky, Thesis Diss. Doct. Chem., Inst. Phys. Chem., Kiev, 1978.
[5] E.I. Andreikov, Yu.A. Sveshnikova and N.D. Rusyanova, Kinet. Catal., 15 (1974) 1207.
[6] V.M. Vorotinzev, Yu.I. Pyatnitsky and G.I. Golodets, Theoret. Exper. Chem., 12 (1976) 488.
[7] G.K. Boreskov, Kinet. Catal., 14 (1973) 7.
[8] V.D. Sokolovsky, in G.K. Boreskov, Editor, Theoretical Problems of Catalysis, Institute of Catalysis, Novosibirsk, 1977, p. 33.
[9] G.I. Golodets, Yu.I. Pyatnitsky and L.N. Raevskaya, Kinet. Catal., 25 (1984) 571.
[10] Yu.I. Pyatnitsky and L.N. Raevskaya, React. Kinet. Catal. Lett., 26 (1984) 173.
[11] A.A. Yabrov and A.A. Ivanov, React. Kinet. Catal. Lett., 14 (1980) 347.
[12] P. Mars and D.W. Van Krevelen, Chem. Eng. Sci., 3 (special supplement) (1954) 41.
[13] D. Vanchove and M. Blanchard, J. Catal., 36 (1975) 6.
[14] M. Blanchard and D. Vanchove, Bull. Soc. Chim. France, 11 (1971) 4134.
[15] A.A. Ivanov and B.S. Balzhinimaev, in Yu.Sh. Matros, Editor, Unsteady-State Processes in Catalysis, VSP BV, Utrecht, 1990, pp. 90–111.
[16] Yu.I. Pyatnitsky, in O.V. Krylov (Editor), Partial Oxidation of Organic Compounds, Nauka, Moscow, 1985, pp. 132–145.
[17] Yu.I. Pyatnitsky, Appl. Catal. A, 113 (1994) 9.
[18] H.W. Zanhoff and M. Baerns, Ind. Eng. Chem. Res., 29 (1990) 2.
[19] W.M.H. Geerts, Q. Chen, J.M.H. van Kasteren and K. van der Wiele, Catal. Today, 6 (1990) 519.
[20] J.C. McCarty, in E.E.Wolf (Editor), Methane Conversion by Oxidative Processes, Van Nostrand Reinhold, New York, 1992, pp. 320–350.
[21] G.S. Lane and E.E. Wolf, J. Catal., 113 (1988) 144.
[22] J.Y. Zhu, R. Dittmayer and H. Hoffman, Chem. Eng. Proc., 32 (1993) 167.
[23] C.A. Mims, R. Mauti, A.M. Dean and K.D. Rose, J. Phys. Chem., 98 (1994) 13357.
[24] Z.S. Andrianova, A.N. Ivanova, P.E. Matkovskii and G.P. Startzeva, Kinet. Catal., 34 (1993) 396.
[25] N.I. Ilchenko and Yu.I. Pyatnitsky, Second Workshop C1–C3 Hydrocarbon Conversion, Krasnoyarsk, Russia, 1994, Abstr., pp. 18–19.
[26] N.I. Ilchenko and Yu.I. Pyatnitsky, in S.T. Oyama, Editor, The Chemistry of Transition Metal Carbides and Nitrides, Chapman and Hall, New York, 1995, pp. 318–324.
[27] W. Tsang and R.F. Hampson, J. Phys. Chem. Ref. Data, 15 (1986) 1087.
[28] J.H. Lunsford, Catal. Today, 6 (1990) 235.